# Acceleration of apatite nucleation on microrough bioactive titanium for bone-replacing implants

**C. Aparicio,[1] J. M. Manero,[1] F. Conde,[2] M. Pegueroles,[1] J. A. Planell,[1] M. Vallet-Regí,[2] F. J. Gil[1]**
[1]*Department of Materials Science and Metallurgical Engineering, E.T.S.E.I.B. Technical University of Catalonia, Avda. Diagonal, 647, Barcelona 08028, Spain*
[2]*Department of Inorganic and Bioinorganic Chemistry, Faculty of Pharmacy, Complutense University of Madrid, Pl. Ramón y Cajal s/n, Madrid 28040, Spain*

Received 20 July 2006; revised 22 September 2006; accepted 3 November 2006
Published online 12 February 2007 in Wiley InterScience (www.interscience.wiley.com). DOI: 10.1002/jbm.a.31164

**Abstract:** The viability of a new two-step method for obtaining bioactive microrough titanium surfaces for bone replacing implants has been evaluated. The method consists of (1) Grit blasting on titanium surface to roughen it; and (2) Thermo-chemical treating to obtain a bioactive surface with bone-bonding ability by means of nucleating and growing an apatite layer on the treated surface of the metal. The aim of this work is to evaluate the effect of surface roughness and chemical composition of the grit-blasting particles on the ability of the surfaces of nucleating and growing a homogeneous apatite layer. The determination and kinetics of the nucleation and growing of the apatite layer on the surfaces has mainly been studied with environmental scanning electron microscopy (ESEM) and grazing-incidence X-ray diffractometry. The results show that $Al_2O_3$-blasted and thermochemically-treated titanium surfaces accelerates nucleation of the apatite, whereas SiC-blasted and thermochemically-treated titanium surfaces inhibits apatite nucleation, compared with the well studied polished and thermochemically-treated titanium surfaces. The acceleration of the apatite nucleation on the $Al_2O_3$-blasted microrough titanium surfaces is because concave parts of the microroughness that are obtained during grit blasting provides to the rough and bioactive surfaces with a chemical- and electrostatic-favored situation for apatite nucleation. This consists of a high density of surface negative charges (also assisted by the nanoroughness of the surface obtained after the thermochemical treatment) and an increased concentration of the $Ca^{2+}$-ions of the fluid, which have a limited mobility at the bottom of the concave parts. © 2007 Wiley Periodicals, Inc. J Biomed Mater Res 82A: 521–529, 2007

**Key words:** apatite nucleation; bioactivity; titanium; grit blasting; topography

## INTRODUCTION

Titanium and some of its alloys are now dominant biomaterials because of their good biocompatibility. Commercially pure titanium (c.p. Ti) implants are alloplastic materials used as the foundation for replacing teeth in dentistry and are also used for orthopaedics.[1] Clinical success of bone-replacing implants, some of them made of c.p. Ti, is obtained when osseointegration is achieved, that is, when the surface of the implant is structurally and functionally joined to the newly-formed bone.[2] The improvement of the short- and long-term osseointegration is a function of a series of factors.[3] Among them, surface quality of the implant (physico–chemical and topographical) is one of the most important. In fact, the entire biological and mechanical interactions between the implant and the surrounding tissues are made at their interface.

In terms of physico–chemical surface quality, it is known that c.p. Ti is biocompatible mainly because of its excellent corrosion behavior in the physiological environment. This is because of the extremely-passive titanium-oxide that spontaneously covers the metal.[2,4] However, c.p. Ti is a bioinert material without bone–bonding ability. The interaction between the metal and the hard tissue does not involve a chemical bond.[5] The lack of ability to bond chemically and the lack of rapid favorable guided reactions lead to an osseointegration process that takes place at a slow rate. In this sense, the so call bio-

*Correspondence to:* C. Aparicio; e-mail: conrado.aparicio@upc.edu
Contract grant sponsor: Ministry of Science of the Spanish Government; contract grant number: MAT2003-08165

active synthetic materials are materials that are able to nucleate and grow on them a layer of apatite (mineral phase of bone) *in vivo*. This allows the bone–bonding ability of the material and its earlier integration in the living tissue. However, these materials are ceramics with inappropriate fracture toughness.

Kokubo et al.[6,7] have demonstrated that an alkali etching (5*M* NaOH) followed by a heat treatment process (600°C, 1 h) makes titanium bioactive by means of the reaction of the NaOH with the $TiO_2$ that naturally covers the metal. This reaction leads to the formation of a dense sodium–titanate gel. An *in vitro* chemically-deposited bone-like apatite layer on c.p. Ti could be induced if the treated surfaces are soaked in a simulated body fluid (SBF). The formation of the apatitic layer is due to electrostatic and ionic interactions between the sodium–titanate surface and the surrounding fluid.[7]

The titanium-surface obtained after the thermochemical treatment can release $Na^+$-ions into the SBF via an ion-exchange reaction with $H_3O^+$-ions, which results in the formation of many Ti-$OH^-$ groups on its surface. These Ti-$OH^-$ groups make a highly negatively-charged surface that initially combine with positive $Ca^{2+}$ ions to form amorphous calcium titanate in the surface environment, and later the calcium titanate combines with the negative phosphate ions to form amorphous calcium phosphate. The amorphous calcium phosphate, at the SBF-pH, eventually transforms into bone-like apatite. These interactions have been also obtained *in vivo*, and smooth titanium implants are soon tightly bonded to the surrounding living bone through the bone-like apatite layer. Consequently, this smooth bioactive c.p. Ti improves the short-term *in vivo* bone reactions.[8]

In terms of topographical quality of the c.p. Ti surface, it is known that an increased implant-surface roughness significantly influence the osteoblastic response *in vitro*.[9,10] Moreover, a better long-term *in vivo* response is achieved when the surface roughness increases since the percentage of implant in direct contact with bone increases as well as loads and torques for extracting implant from bone.[11]

Grit blasting, which consists of bombarding a surface with a myriad of small abrasive biologically-inert ceramic particles, is one of the most frequently used treatments for obtaining a rough surface of a metal implant.[12] The surface treatment forces different surface roughness mainly depending on the size of the particles used. In previous works, a biologically-beneficial cell response has been determined when blasting with a 600-μm particle-size that results in a surface roughness of $R_a$ (4–5 μm).[13] However, the adhesion of parts of the particles on the implant surface because of the high-velocity impact may change physico-chemical surface quality.[14,15] This fact can influence on all the reactions and interactions at the surface of the metal. The particles that remain adhered on the surface can not be removed, even after ultrasonical cleaning.

In this study, the viability of a new two-step method for obtaining bioactive microrough titanium surfaces has been evaluated to get a metal surface with an excellent long-term osseointegration (because of the microroughness) and a rapid short-term osseointegration (because of its bioactive properties). This new treatment consists of: (1) grit blasting the titanium surface to roughen it; and (2) thermo-chemical treatment, developed by Kokubo et al.,[6] to obtain a bioactive surface with bone–bonding ability.

An interference of grit blasting in the electrostatic and ionic interactions that leads to the formation of the apatite layer on the c.p. Ti after the thermochemical treatment can be expected. This interference can be due to the microroughness as well as to the surface chemical heterogeneities produced by the parts of the grit particles that remain adhered.

The aim of this work is to evaluate the *in vitro* bioactivity of rough and bioactive titanium surfaces obtained by a blasting + thermochemical-treatment method, that is, to study the effect of surface roughness and chemical composition of the grit blasting particles on the ability of the surfaces of nucleating and growing a homogeneous apatite layer.

## MATERIALS AND METHODS

### Materials and surface treatments

$10 \times 10$-$mm^2$ c.p. Ti Grade III plaques were treated with six different surface treatments:

Ti: 1 μm-alumina polishing.

AL6: grit blasting with $Al_2O_3$-particles of 425–600 μm in size. Grit blasting was done at 2.5 MPa of pressure.

SI6: grit blasting with SiC-particles of 425–600 μm in size. Grit blasting was done at 2.5 MPa of pressure.

Ti-Bio: Ti + thermochemical treatment. The thermochemical treatment was done according to Kokubo et al.[6] This treatment consists of: (1) Introducing the plaque into a vial containing 10 ml of 5*M*-NaOH. The vial is placed in an oven at 60°C during 24 h. (2) Careful rinsing during 30 min in 100 mL of distilled water. (3) Drying at 40°C in an oven during 24 h. (4) Thermal treating in a tubular furnace in air up to 600°C with a 5°C/min heating-rate, and maintenance during 1 h. (5) Cooling inside the furnace down to room temperature.

AL6-Bio: AL6 + thermochemical treatment.

SI6-Bio: SI6 + thermochemical treatment.

Each plaque was introduced into a vial containing 40 mL of SBF,[16] and placed in an oven at 37°C during 11 days to perform the *in vitro* testing of their bioactivity. Every three days the solution was renewed. Ten plaques per each surface treatment were analysed.

### Environmental scanning electron microscopy

The observation of the evolution of the species that grew on the c.p. Ti surfaces was performed by means of an environmental scanning electron microscope (ESEM) (2020©, Electroscan).

The ESEM does not need to operate neither under vacuum nor with electron-conductor surfaces. These properties allow following the evolution of the same sample throughout the 11 days of immersion in SBF, as demonstrated in a previous work.[17]

Different samples of every surface treatment were observed during all of the 1–5 days of immersion in SBF, and at the end of the study (day 11).

### Grazing-incidence X-ray diffraction

The chemical species nucleated and grown on the c.p. Ti surfaces were analyzed by grazing-incidence X-ray diffraction (GI-XRD) in an automatic diffractometer (X'Pert MPD©, Philips, The Netherlands) equipped with a thin film attachment, using Cu-$K_\alpha$ radiation.

A range of $2\theta = 20$–$50^\circ$ was studied in continuous mode, under a fixed incidence angle of $\theta_f = 0.5^\circ$. A step size of $0.02^\circ$ was used in all scans, with a 2 s-time per step. To improve the signal to noise ratio, the AL6-Bio surfaces were also analyzed in step mode with a time per step of 10 s all along the period of immersion in SBF.

Samples before being immersed in SBF, and after 3, 5, and 11 days of immersion were analyzed.

### Profilometry

Quantitative surface-roughness of the surfaces was determined before and after the immersion into the SBF.

Surface profiles ($P$) were obtained with a contact 2D-profilometer (Surftest SV500©, Mitutoyo, Japan) and roughness profiles ($R$) were calculated by filtering P-profiles with a Gaussian filter. A 0.8-mm "cut-off" value was applied for filtering.

$R_a$ and $P_c$, a vertical and a horizontal surface-roughness parameter, respectively, were calculated from the R-profiles with appropriate software (Surfpack$^{TM}$ v3.00, Mitutoyo, Japan), according to international standards (ISO4287: 1997).

### Streaming potential

A streaming potential instrument (Electrokinetic Analyzer-EKA©, Anton Paar, Austria) with an asymmetric clamping cell was used to determine apparent Z-potential of the flat surfaces ($\zeta$).

The "titration unit" allowed automatically-performed series of measurements at a varied-pH solution. A 1-m$M$ KCl solution was used as electrolyte. The pressure ramp was run up to a maximum pressure of 600-mbar. The electrolyte solution was adjusted to a starting pH = 9.0, using 0.1$M$ NaOH. The automatic titration was performed down to pH = 3.0, adding 0.1$M$ HCl.

### Statistics

$t$-Student tests were done with an appropriate software (Minitab$^{TM}$ Release 13.1, Minitab) to evaluate the statistically significance of the differences between the roughness mean-values obtained.

## RESULTS

### Bioactivity

Figure 1 shows the morphology of the different c.p. Ti surfaces, before being immersed in SBF, without and with thermochemical treatment (Ti, SI6, AL6; Ti-Bio; SI6-Bio, AL6-Bio).

The grit-blasted surfaces that were not thermochemically treated (AL6, SI6) show a random non-texturized roughness with parts of the grit particles adhered on them (Fig. 1, centre- and right-up). Plastic deformation produced during polishing can be seen on Ti-surfaces (Fig. 1, left-up).

All the thermochemically-treated surfaces (Ti-Bio, AL6-Bio, and SI6-Bio) show a skeletal nanoporous structure that is superimposed on the microroughness obtained with the previous treatment (blasting or polishing) (Fig. 1, down). The parts of the grit particles that remain on the blasted surfaces are also totally, on SI6-Bio surfaces (Fig. 1, centre-down), or partially, on AL6-Bio surfaces (Fig. 1, right-down), covered by the nanoporous structure.

Figure 1-up also shows an example of GI-XRD for each of the surfaces that were not thermochemically treated. The three main maxima of these surfaces correspond to titanium (JCPDS no. 44-1294). Rutile maxima (JCPDS no. 21-1276) are also present in some of these surfaces. Diffraction maxima corresponding to either $Al_2O_3$ or SiC were not detected at the grit-blasted surfaces.

The GI-XRD of a Ti-Bio surface shows titanium and rutile maxima as well as three more maxima that correspond to two different sodium-titanate stoichiometries, $Na_2Ti5O_{11}$ (JCPDS no. 11-0289) and $NaTiO_2$ (JCPDS no. 16-0251) (Fig. 1, left-down). Sodium-titanate and rutile maxima where not observed when the X-ray diffraction patterns were performed under Bragg-Brentano (theta-2 theta) conditions (not shown), which confirms the superficial character of these species. The GI-XRD patterns of AL6-Bio and SI6-Bio surfaces are also shown in Figure 1-down (centre and right). The sodium-titanate maxima do not appear so clearly as in Ti-Bio surfaces because the significant roughness of these surfaces leads to a pattern with a higher background.

During the 2-first days of immersion in SBF none of the studied c.p. Ti surfaces show any crystalline or cover growing on them. However, at day 3 some

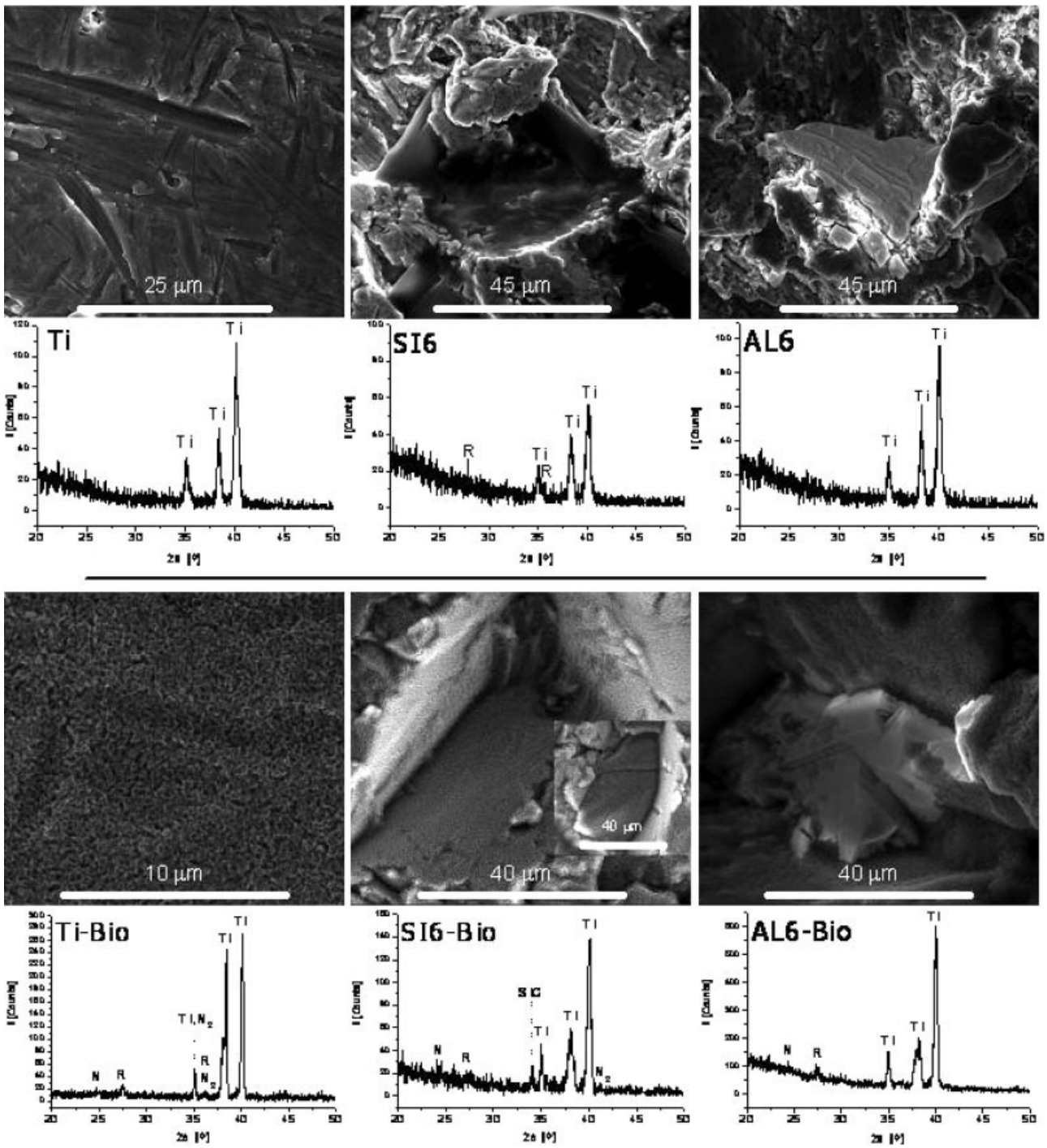


**Figure 1.** ESEM pictures and GI-XRD of Ti (left-up), SI6 (centre-up), AL6 (right-up), Ti-Bio (left-down), SI6-Bio (centre-down), and AL6-Bio (right-down) surfaces. Ti, titanium; R, $TiO_2$-rutile; N, $Na_2Ti_5O_{11}$; $N_2$, $NaTiO_2$; SiC, SiC.

crystalline nuclei were detected by ESEM on the AL6-Bio surfaces (Fig. 2). The nuclei were spherical-like with 2–5 μm in diameter, formed by agglomerates of nanometric crystals. None of the other surfaces showed this crystalline nucleation at day 3.

At day 4, the AL6-Bio surfaces were homogenously covered with a continuous layer of crystalline agglomerates (Fig. 3) of the type shown in Figure 2. According to the GI- XRD of the $Al_2O_3$-blasted and thermochemically treated surfaces (Fig. 3, right-down), the wide and weak maxima around $2\theta = 30.5–33^\circ$ and $26^\circ$ are compatible with a poorly crystalline apatite (JCPDS no. 09-0432). Other relevant result is that the layer of apatitic agglomerates reproduces the original topography of the surface, preserving the roughness at the micrometer level. A

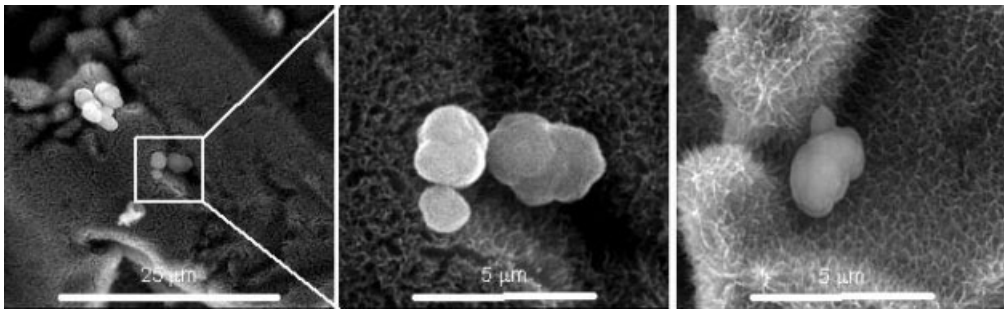


**Figure 2.** ESEM pictures showing crystalline (apatite) nuclei on the AL6-Bio surfaces after 3 days of immersion in SBF.

maximum corresponding to the remaining $Al_2O_3$-particles (JCPDS no. 46-1212), that was not detected in the patterns shown in Figure 1, could be detected because of the higher number of counts obtained in this GI-XRD pattern. Among all the other surfaces neither crystalline nucleation nor covering after 4 days of immersion in SBF were observed.

At day 5, the Ti-Bio surfaces were also completely covered by the apatitic layer (Fig. 4); whereas all the other c.p. Ti surfaces, including the SI6-Bio, did not have this covering.

Finally, at day 11 (Fig. 5), there were no changes in all the different surfaces compared with day 5. Consequently, the SI6-Bio surfaces, that is, SiC-blasted and thermochemically-treated, inhibits the growing of the apatite layer (Fig. 5, right). The GI-XRD of these surfaces after 11 days in SBF is analogous to that obtained before immersing them in SBF.

The GI- XRD patterns of Ti-Bio (Fig. 5, left) and AL6-Bio surfaces (Fig. 5, centre), after 11 days in SBF show maxima at $2\theta = 30.5–33^\circ$ and $25.9^\circ$, which confirms the apatitic nature of the layer.

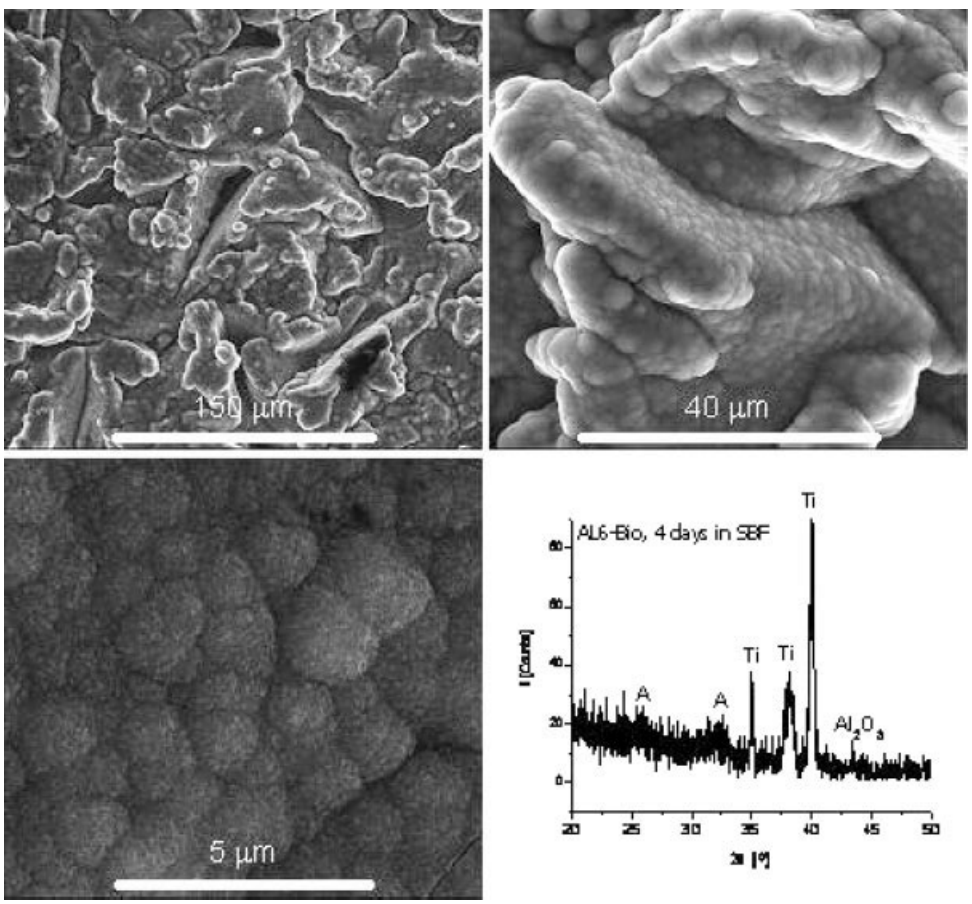


**Figure 3.** ESEM pictures showing a continuous and homogeneous crystalline (apatite) layer on the AL6-Bio surfaces after 4 days of immersion in SBF, including GI-XRD of these surfaces. Ti, titanium; A, apatite; $Al_2O_3$, $Al_2O_3$.

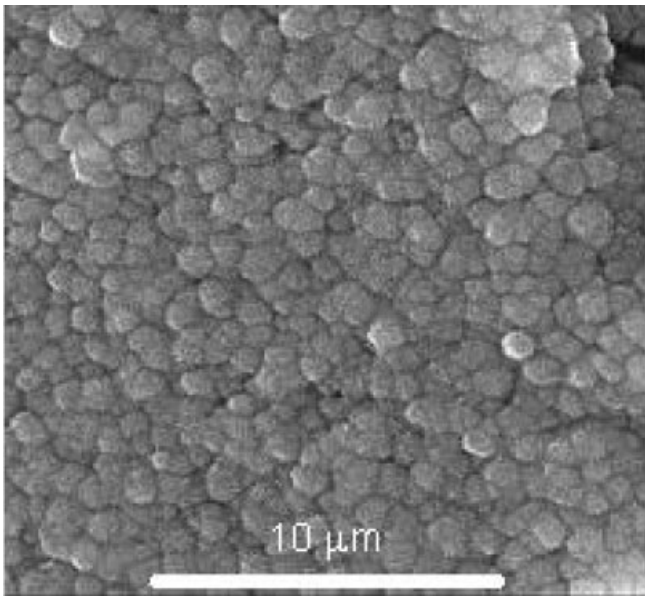


**Figure 4.** ESEM picture showing a continuous and homogeneous crystalline (apatite) layer on a Ti-Bio surface after 5 days of immersion in SBF.

### Roughness

Table I summarizes the results of surface roughness. There are no statistically significant differences between the values for c.p. Ti with or without thermochemical treatment and the same previous surface treatment.

Moreover, there are no statistically significant differences between the mean roughness parameters of the different c.p. Ti surfaces before and after 11 days of immersion in SBF, except for the Ti-Bio samples. Ti-Bio surfaces have a significantly higher $R_a$ and a lower $P_c$ after 11 days in SBF.

### Zeta-potential

Figure 6 shows the evolution of ζ-values depending on pH for Ti-Bio and AL6-Bio surfaces. The higher the pH, the lower the ζ. The values and evolution of ζ is very similar for Ti-Bio and AL6-Bio up to pH = 4. At higher pH, ζ is significantly lower for Ti-Bio than for AL6-Bio surfaces.

## DISCUSSION

The thermochemical treatment produces a homogeneous skeletal nanoporous structure on the polished as well as on the grit-blasted surfaces (Fig. 1, down). According to the GI-XRD patterns, the nanoporous structure is a sodium titanate in all the thermochemically-treated surfaces (Fig. 1, down). Two different stoichiometries of the titanate were detected; $Na_2Ti_5O_{11}$, which has been previously referenced by Kokubo et al.,[6] and $NaTiO_2$, which has other relevant maxima overlapped with some maxima of

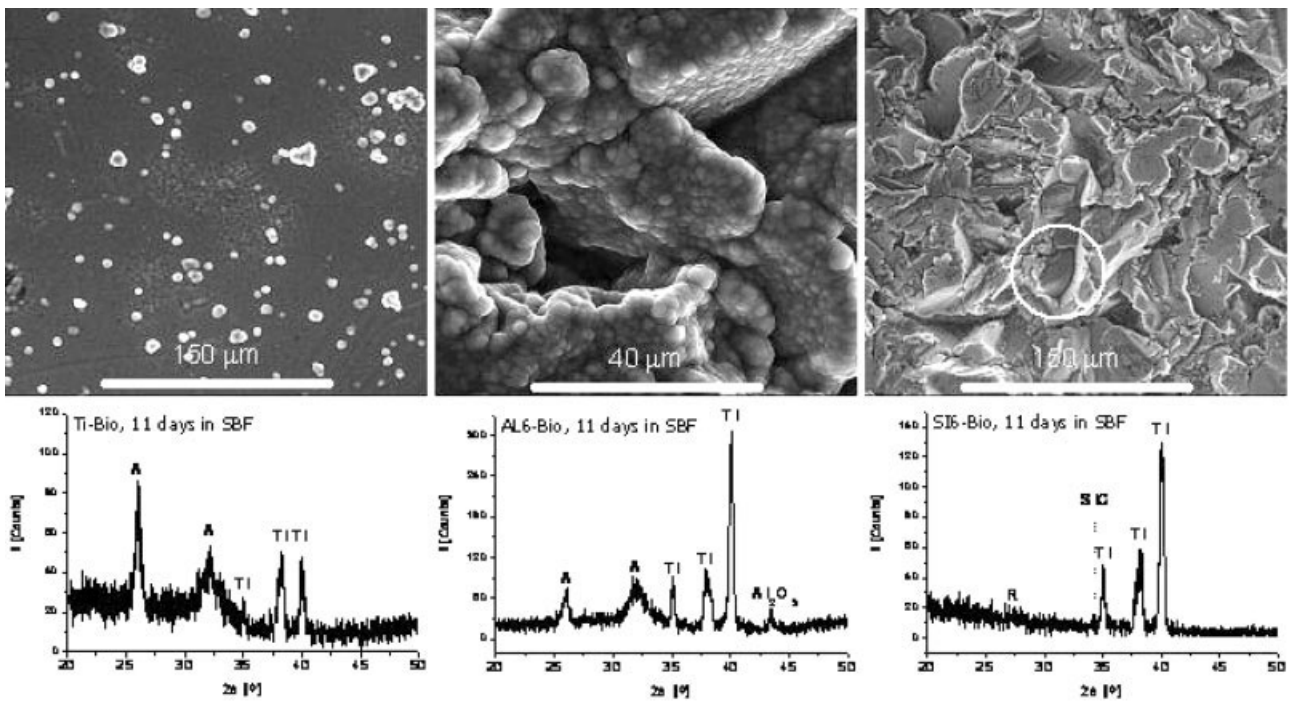


**Figure 5.** ESEM pictures and GI-XRD of Ti-Bio (left), AL6-Bio (centre), and SI6-Bio (right) surfaces after 11 days of immersion in SBF. Note that the circled particle on the SI6-Bio surface is the same as in Figure 3 (down-left). Ti, titanium; A, apatite; $Al_2O_3$, $Al_2O_3$; R, $TiO_2$-rutile; SiC, SIC.

**TABLE I**
**Mean-Roughness Values of the Different c.p. Ti Surfaces, Before and After Being Immersed in SBF During 11 Days**

| | Before Immersing in SBF | | After 11 Days Immersed in SBF | |
|---|---|---|---|---|
| | $R_a \pm$ S.D. [μm] | $P_c \pm$ S.D. [$cm^{-1}$] | $R_a \pm$ S.D. [μm] | $P_c \pm$ S.D. [$cm^{-1}$] |
| Ti | 0.07 ± 0.02 | 154.6 ± 77.9 | 0.08 ± 0.02 | 212.9 ± 78.9 |
| Ti-Bio | 0.09 ± 0.01 | 190.9 ± 56.2 | 0.38 ± 0.16 | 139.9 ± 56.2 |
| AL6 | 4.15 ± 0.26 | 76.1 ± 21.5 | 4.22 ± 0.31 | 81.1 ± 12.5 |
| AL6-Bio | 4.23 ± 0.21 | 92.1 ± 33.7 | 4.54 ± 0.33 | 75.3 ± 22.4 |
| SI6 | 3.59 ± 0.21 | 87.3 ± 11.5 | 3.84 ± 0.24 | 78.8 ± 26.3 |
| SI6-Bio | 3.62 ± 0.16 | 99.6 ± 21.4 | 3.55 ± 0.22 | 82.8 ± 19.8 |

S.D., Standard deviation.

titanium and rutile. The intensity of the maxima of the titanate is significantly lower in the blasted surfaces because the roughness, in the range of $R_a \approx$ 4–5 μm (Table I), induces a higher background. This is despite the GI- XRD of AL6-Bio and SI6-Bio surfaces were obtained with a higher number of counts per time-step, which confirms the superficial character of the titanate.

After being immersed in SBF, the different c.p. Ti surfaces have shown different responses. Whereas most of the surfaces (Ti, AL6, SI6, and SI6-Bio) did not show any change during the eleven days of the study, the Ti-Bio and AL6-Bio have led to the growing of a crystalline-apatite layer on them. However, the kinetics of the nucleation of the layer was also different. The nucleation of the apatite on AL6-Bio surfaces was detected after 3 days of immersion in SBF (Fig. 2), and after 4 days the surfaces were completely covered by the crystalline agglomerates (Fig. 3), which are apatite, as confirmed by GI-XRD (Fig. 3). The Ti-Bio surfaces were completely covered by the layer one day after, that is, at day 5 (Fig. 4). The nucleation stage was not detected in Ti-Bio surfaces, despite the use of ESEM, which indicates that once the nucleation occurs the subsequent growing of the layer proceeds spontaneously and rapidly. The crystals obtained are nanometric, as confirmed and quantified by means of TEM by other authors.[18,19]

Figure 5-left shows that the maximum at $2\theta = 25.9^\circ$, corresponding to the (00.2)-planes of apatite, is the main one for Ti-Bio surfaces. However, apatites have the main maxima at $2\theta = 31.8^\circ$, which corresponds to their (21.1)-planes. Consequently, a (00.2) preferential structural growing is obtained on Ti-Bio surfaces. In the case of Al6-Bio there is also a clear indication of the favored orientation of growing for the (00.2)-planes because the ratio of the relative strength of the apatite (0.02)-planes to the apatite (21.1)-planes is about 0.9, whereas that of the standard apatite is 0.4 (JCPDS no. 09-0432) (Fig. 5, centre). This can be done because of an epitaxial growing of the apatite on the c.p. Ti by means of the matching of the structure of crystal planes in c.p. Ti and the apatite formed.[20] It has been proposed that the structure of rutile (101) is matching to the structure of apatite (00.4), which is parallel to the (00.2) crystal plane structure.[21]

The acceleration of the nucleation of the apatite layer on the AL6-Bio surfaces can have different causes, that is, because of (1) the particles, (2) the roughness, or (3) the particles and the roughness. An ~15% of titanium surface covered by the remaining alumina particles was previously determined.[15] Alumina, unlike titania, is positively charged when immersed in SBF[22] because its isoelectric point (IEP = 7.8) is higher than the pH of SBF (pH = 7.4). Consequently, the alumina particles attached to the AL6-Bio surfaces (Fig. 1, right-down) make these surfaces less negatively charged in the SBF. This is confirmed by the results of apparent zeta-potential (Fig. 6), where, at pH = 7.4, $\zeta$ is approximately −5 mV for AL6-Bio surfaces and −13 mV for Ti-Bio surfaces. The negative charge on the thermochemically-treated surfaces is provided by the formation of Ti-$OH^-$ groups. These hydroxyl groups, according

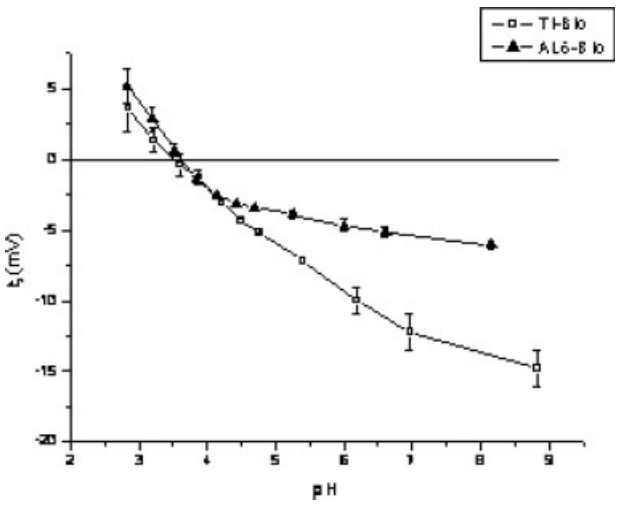


**Figure 6.** Apparent zeta-potential ($\xi$) versus pH for Ti-Bio (□) and AL6-Bio (▲) surfaces.

to Kokubo et al.,[23] are needed in abundance to get the formation on the treated surfaces of an amorphous calcium-titanate that eventually will combine with phosphates to, finally, crystallize as apatite. Consequently, the presence of the $Al_2O_3$-particles on the surface is far from accelerating the nucleation of the aptatite (bioactivity) on AL6-Bio surfaces.

However, the increased roughness at the micrometer level can explain this acceleration. It is known that nanometric spaces of the organic matrix with distributions of highly-negative charges are needed for the nucleation of the biologic minerals, such as apatite.[24] According to this, the skeletal nanoporous structure of the sodium-titanate gives and ideal electrostatic situation for the nucleation of the apatite. Moreover, Wang et al.[25] concluded that apatite nucleation is favored in that parts of the surface where, as a consequence of macroscopic geometric features, ionic concentration on titanium surface is higher. All these studies confirm that surface topography and charge as well as the ionic concentration in the solution nearest the metal surface influence apatite nucleation. The AL6-Bio surfaces have a real surface increased by both micro- and nano-roughness. The nanoroughness provides the thermochemical-treated surfaces with a signitificative amount of hydroxyl groups, which are essential for apatite nucleation, as explained before. Despite the roughness at the micrometer level also should increase the amount of hydroxyl groups because of the increased real surface area, it is not enough to compensate the effect of the attached $Al_2O_3$-particles on the net charge of the surface (Fig. 6). However, ESEM pictures show that the apatite nucleation on AL6-Bio was preferentially at the concave parts of the microtopography (Fig. 2). Concave parts not only are more reactive (residual stresses are higher because these parts directly receive the particle impacts) but also favor the concentration of more negative surface-charges and more ions from the solution because of their morphology (V-shape). The mobility of the ions in the SBF at the concave parts of the rough surfaces is restricted because these parts provoke a well-effect, and the V-shape of the concave parts significantly concentrates the negative charges on the surroundings of their bottoms.

As a consequence of all these comments, the acceleration of the nucleation of the apatite on the AL6-Bio surfaces is attributed to the surface topographical changes at the micrometer level of these blasted-rough c.p. Ti materials.

Not only the roughness but also the chemical nature of the grit blasting particles can influence the bioactivity of the blasted c.p. Ti surfaces because SI6-Bio surfaces inhibits the growing of the apatite layer. Taking into consideration that the only significant difference between AL6-Bio and SI6-Bio surfaces is the different surface chemical heterogeneity—topography is quantitatively and qualitatively equivalent (Fig. 1 and Table I)—the inhibition of the bioactive behavior of the SiC-blasted surfaces may be a consequence of the reaction of the particles with the atmosphere of the furnace. As a result of this expected reaction, carbonates may form, which may interfere or modify the electrostatic equilibriums needed for the apatite nucleation. However, to confirm it further studies should be performed.

It is important to note that others have studied the mechanical properties of the titanate gel[26] and the c.p. Ti[27] after the thermochemical treatment is performed. Despite the atmosphere inside the furnace was not controlled, the adherence of the titanate gel was improved and the fatigue resistance of the metal, which is the main mechanical property for its adequate long-term performance, was not negatively affected.

Figure 5-left shows a new stage of nucleation on an already-formed apatite layer. Moreover, the intensity of the apatite maxima in the GI-XRD pattern of AL6-Bio after 11 days of immersion in SBF (Fig. 5, centre) is significantly higher than after 4 days in SBF (Fig. 3). These two results confirm that the layer of apatite both on Ti-Bio and on AL6-Bio increased its thickness throughout the time of immersion in SBF.

This growing of the apatite layer has not modified the original roughness of the rough and bioactive surfaces. $R_a$ and $P_c$ have no statistically significant differences before and after the growing of the apatite layer (Table I). This result is important in terms of the clinical goal of the surface treatment applied on the c.p. Ti surfaces because the surface is bioactive, as demonstrated here, and the surface also have the microroughness for an optimal biological response.[11] Consequently, these rough and bioactive surfaces can get an adequate long-term osseointegration and a significantly enhanced short-term integration in the surrounding hard-tissues.

## CONCLUSIONS

Grit blasting influences the bioactivity of the thermochemically-treated c.p. Ti surfaces. The rough and thermochemically treated $Al_2O_3$-blasted surfaces (AL6-Bio) accelerate the bioactive apatite-layer formation, whereas the rough and thermochemically-treated SiC-blasted surfaces (SI6-Bio) inhibited the bioactivity, compared with the well-studied polished and thermochemically-treated c.p. Ti surfaces (Ti-Bio).

The concave parts of the microroughness that are obtained during grit blasting provides to the rough and bioactive surfaces with a chemical- and electrostatic-favored situation for apatite nucleation. As a consequence, an earlier apatite nucleation is obtained on these surfaces.

This earlier nucleation may be related with a significantly enhanced short-term integration in the surrounding hard-tissues because the *in vivo* apatite-layer formation will be accelerated and, consequently, the osseointegration process will also be accelerated.

The authors acknowledge Dr. Ana Cordeiro and Prof. Mario Barbosa from the Instituto Nacional de Engenharia Biomédica in Porto, Portugal, for their help in the zeta-potential measurements.

## References

1. Carlsson SL, Rostlund TR, Albrektsson B, Albrektsson T, Brånemark P-I. Osseointegration of titanium implants. Acta Orthop Scand 1986;57:285–289.
2. Brånemark P-I, Hansson BO, Adell R, Breine U, Lindström J, Hallen O, Öhman A. Osseointegrated implants in the treatment of edentulous jaw. Experience from a 10-year period. Scand J Plast Reconstr Surg 1977;11 (Suppl 16):1–132.
3. Albrektsson T, Brånemark P-I, Hansson HA, Lindström J. Osseointegrated titanium implants. Acta Orthop Scand 1981; 52:155–170.
4. Pourbaix M. Electrochemical corrosion of metallic biomaterials. Biomaterials 1984;5:122–134.
5. Sennerby L, Thomsen P, Ericson LE. Early tissue response to titanium implants inserted in rabbit cortical bone. II. Ultrastructural observations. J Mater Sci: Mater Med 1993;4:494–502.
6. Kokubo T, Miyaji F, Kim HM. Spontaneous formation of bonelike apatite layer on chemically treated titanium metals. J Amer Ceram Soc 1996;79:1127–1129.
7. Kokubo T, Kim HM, Kawashita M, Nakamura T. Bioactive metals: preparation and properties. J Mater Sci: Mater Med 2004;15:99–107.
8. Kokubo T, Miyaji F, Kim HM, Nakamura TJ. Bonding strength of bonelike apatite layer to Ti metal substrate. Biomed Mater Res (Appl Biomater) 1997;38:121–127.
9. Anselme K. Osteoblast adhesion on biomaterials. Biomaterials 2000;21:667–681.
10. Boyan BD, Lohmann CH, Dean DD, Sylvia VL, Cochran DL, Schwartz Z. Mechanisms involved in osteoblast response to implant surface morphology. Annu Rev Mater Res 2001;31: 357–371.
11. Buser D. Titanium for dental applications (II): Implant with roughened surfaces. In: Brunette DM, Tengvall P, Textor M, Thomsen P, editors. Titanium in Medicine: Material Science, Surface Science, Engineering, Biological Responses and Medical Applications. Berlin: Springer–Verlag; 2001. pp 875–885.
12. Jones FH. Teeth and bones: Applications of surface science to dental materials and related biomaterials. Surf Sci Rep 2001; 42:75–205.
13. Aparicio C, Engel E, Gil FJ, Planell JA. Human-osteoblast proliferation and differentiation on grit-blasted and bioactive titanium for dental applications. J Mater Sci: Mater Med 2002; 13:1105–1111.
14. Placko HE, Mishra S, Weimer JJ, Lucas LC. Surface characterization of titanium-based implant materials. Int J Oral Maxillofac Implants 2000;15:355–363.
15. Aparicio C, Gil FJ, Fonseca C, Barbosa M, Planell JA. Corrosion behaviour of commercially pure titanium shot blasted with different materials and sizes of shot particles for dental implant applications. Biomaterials 2003;24:263–273.
16. Kokubo T, Kushitani H, Sakka S, Kitsugi T, Yamamuro T. Solutions able to reproduce in vivo surface-structure changes in bioactive glass-ceramic A-W[3]. J Biomed Mater Res 1990; 24:721–734.
17. Gil FJ, Padrós A, Manero JM, Aparicio C, Nilsson M, Planell JA. Growth of bioactive surfaces on titanium and its alloys for orthopaedic and dental implants. Mater Sci Eng C 2002; 22:53–60.
18. Takadama H, Kim HM, Kokubo T, Nakamura T. TEM-EDX study of mechanism of bonelike apatite formation on bioactive titanium metal in simulated body fluid. J Biomed Mater Res 2001;57:441–448.
19. Leng Y, Lu X, Chen J. Identifying calcium phosphates formed in simulated body fluid by electron diffraction. Key Eng Mater 2004;254–256:339–342.
20. Bryan MC. Crystal structure of cholesterol monohydrate. Nature 1976;260:727–729.
21. Yang B, Uchida M, Kim HM, Zhang X, Kokubo T. Preparation of bioactive titanium metal via anodic oxidation treatment. Biomaterials 2004;25:1003–1010.
22. Li P, Ohtsuki C, Kokubo T, Nakanishi K, Soga N, Nakamura T, Yamamuro T, de Groot K. The role of hydrated silica, titania, and alumina in inducing apatite on implants. J Biomed Mater Res 1994;24:7–15.
23. Kokubo T, Kim HM, Kawashita M. Novel bioactive materials with different mechanical properties. Biomaterials 2003;24: 2161–2175.
24. Heuer AH, Fink DJ, Laraia VJ, Arias JL, Calvert PD, Kendall K, Messing GL, Blackwell J, Ricke PC, Thomson DH, Wheeler AP, Veis A, Caplan AI. Innovative materials processing strategies: A biomimetic approach. Science 1992;255:1098–1105.
25. Wang XX, Hayakawa S, Tsuru K, Osaka A. A comparative study of in vitro apatite deposition on heat- $H_2O_2$-, and NaOH-treated titanium surfaces J Biomed Mater Res 2001;54: 172–178.
26. Kim HM, Miyaji F, Kokubo T, Nakamura T. Effect of heat treatment on apatite forming ability of Ti metal induced by alkali treatment. J Mater Sci: Mater Med 1997;8:341–347.
27. Kim HM, Saaki Y, Suzuki J, Fujibayashi S, Kokubo T, Matsushita T, Nakamura T. Mechanical properties of bioactive titanium prepared by chemical treatment. Key Eng Mat 2000:191/192:227–230.